# Structure, magnetic properties, and magnetocaloric effect of polycrystalline Ho<sub>3</sub>M (M = Rh, Ru) alloys

Yafen Shang<sup>1, 4</sup>, Yue Yuan<sup>2</sup>, Yutao Cao<sup>1</sup>, R. L. Hadimani<sup>3</sup>, Yurij Mozharivskyj<sup>4</sup>, Hao Fu<sup>1\*</sup>

#### **Abstract**

The structure, magnetic properties, and magnetocaloric effect (MCE) of polycrystalline Ho<sub>3</sub>M (M = Rh, Ru) compounds have been investigated by X-ray diffraction and magnetization measurements. The stoichiometric Ho<sub>3</sub>Rh sample contains two phases Ho<sub>3</sub>Rh and Ho<sub>7</sub>Rh<sub>3</sub>. Two successive magnetic transitions near 34 and 22 K from the Ho<sub>3</sub>Rh and Ho<sub>7</sub>Rh<sub>3</sub> phases, respectively, are observed. The maximum magnetic entropy change ( $-\Delta S_{\rm M}$ ) and refrigerant capacity (RC) of the ascast Ho<sub>3</sub>Rh alloy are 10.0 J/kg K and 320 J/kg, respectively, for the magnetic field change of 50 kOe. For Ho<sub>3</sub>Ru sample, three phases, Ho<sub>3</sub>Ru, Ho<sub>5</sub>Ru<sub>2</sub>, and trace of Ho<sub>2</sub>O<sub>3</sub>, are present. Only one Neel transition temperature was observed near 14 K in the multiple-phase sample. The maximal values of  $-\Delta S_{\rm M}$  are found to be 5.1 J/kg K

<sup>&</sup>lt;sup>1</sup> School of Physics, University of Electronic Science and Technology of China, Chengdu, 610054, People's Republic of China

<sup>&</sup>lt;sup>2</sup> Glasgow College, University of Electronic Science and Technology of China, Chengdu, 611731, People's Republic of China

<sup>&</sup>lt;sup>3</sup>Department of Mechanical and Nuclear Engineering, Virginia Commonwealth University, Richmond VA 23284, USA

<sup>&</sup>lt;sup>4</sup> Department of Chemistry and Chemical Biology, Brockhouse Institute of Materials Research, McMaster University, 1280 Main Street West, Hamilton, Ontario, L8S 4M1, Canada

<sup>\*</sup> Author to whom correspondence should be addressed: fuhao@uestc.edu.cn

around  $T_N$  and the value of RC is estimated to be 145 J/kg for  $\Delta H = 50$  kOe, which is less than that of the Ho<sub>3</sub>Rh sample due to the dominant antiferromagnetic interaction. The excellent magnetocaloric performance indicates the applicability of Ho<sub>3</sub>Rh as an appropriate candidate for magnetic refrigerant in low temperature ranges.

Keywords: Magnetocaloric effect; Magnetic entropy change; Rare earth-transition metal compounds

#### 1. Introduction

The magnetocaloric effect (MCE) is a class of phenomena where a reversible temperature change occurs when the magnetic materials are exposed to an alternating magnetic field <sup>[1,2]</sup>. The magnetic refrigeration technology based on the MCE can achieve cooling in a more energy-efficient and environmentally friendly way <sup>[3]</sup>. Compared with the present gas-compression-based refrigeration technology, magnetic refrigeration has been heralded by academia and industry as the next-generation cooling technique <sup>[4]</sup>.

In recent years, many efforts have been made to explore advanced magnetic refrigerant materials that possess not only a large value of magnetic entropy change  $(\Delta S_M)$  but also a considerable magnetic refrigerant capacity (RC) [5.6]. Pecharsky and Gschneidner [7] discovered the giant MCE (GMCE) in the  $Gd_5(Si_xGe_{1-x})_4$   $(0 \le x \le 0.5)$  alloy series with first-order transitions. It was explained that the coupling of the structural and magnetic phase transitions is responsible for the GMCE. Beside  $Gd_5(Si_xGe_{1-x})_4$  series,  $LaFe_{13-x}Si_x$  [8],  $MnAs_{1-x}Sb_x$  [9],  $MnFeP_{1-x}As_x$  [10] (Mn-Fe-Si-P [11]), Ni-Mn-Ga [12,13],  $Ni_{0.5}Mn_{0.5-x}Sn_x$  [14] etc., also exhibit GMCE around their transition temperatures. The GMCE of those compounds strongly stimulated the study of many other rare earth rich materials of the  $R_3M$  family (R = rare earths, M = transition) metals) because it has the highest R/M ratio within the  $R_xM_y$  intermetallic compound family, which is beneficial to obtain a remarkable MCE [15]. Recently, large MCE were found in  $Gd_3M$  (M = Co, Ni, Rh, and Ru) [16.17,18],  $Tb_3M$  (M = Co, Rh, and Ru)

[15,19,20], and Dy<sub>3</sub>M (M=Co) [21].

The electronic structure, electrical resistivity, lattice parameters, thermal variations and magnetic properties of the intermetallic compound Ho<sub>3</sub>Rh single crystals were extensively examined by E. Talik and coworkers <sup>[22]</sup>. Ho<sub>3</sub>Rh crystallizes in an orthorhombic Fe<sub>3</sub>C-type crystal structure with the space group *Pnma*. It was revealed that Ho<sub>3</sub>Rh single crystal has canted magnetic structure with dominant ferromagnetic interaction and possesses anisotropic magnetic properties along [100], [010], and [001] principal directions. It orders ferromagnetically near 35 K along [100] direction. However, an antiferromagnetic ordering with asymmetric peak can be observed in the thermal variations of the magnetization along both [010] and [001] directions when the applied field is lower than 5 kOe. In addition, a spin reorientation can be observed from the thermal magnetization curves and the occurring temperature is lower than 25 K and varies for different crystalline directions.

Ho<sub>3</sub>Ru also crystallizes in the Fe<sub>3</sub>C-type structure <sup>[23]</sup>. Quit few researches were reported about its magnetic properties except for the large low temperature specific heat in the antiferromagnetic state below 15 K, which can be used as the regenerator material for the GM refrigerator <sup>[24]</sup>.

The aim of this work is to study the structure and MCE of the polycrystalline Ho<sub>3</sub>M (M = Rh and Ru) intermetallic compounds. The large content of rare earth in the compounds may cause remarkable changes in the magnetization near the ordering temperature and generate a noticeable MCE. Additionally, in the Ho-Rh and Ho-Ru binary diagrams, Ho<sub>3</sub>Rh solidifies congruently from the melt and no decomposition

can be observed; however, Ho<sub>3</sub>Ru is formed through the peritectic reaction of the Ho<sub>5</sub>Ru<sub>2</sub> and the melt. In this work, structural analysis is performed on the as-cast polycrystalline Ho<sub>3</sub>Rh and Ho<sub>3</sub>Ru and the results suggests that it is difficult to obtain single phase structure for the compounds. Magnetic measurements are also carried out and the MCE is characterized from the isothermal magnetization.

### 2. Experimental details

Samples examined in this work were prepared by melting materials (99.9 wt.% Ho, 99.99 wt.% Rh, 99.95 wt.% Ru) purity in an arc furnace. In order to ensure the homogeneity of the samples, the ingots were turned upside-down and melted four times. The weight loss after arc melting was negligible. Experimental powder x-ray diffraction (XRD) pattern was collected for  $2\theta = 17\text{-}100^\circ$  with step size of 0.0084° on a PANalytical X'Pert Pro diffractometer with a linear X'Celerator detector using Cu  $K_{a1}$  radiation at room temperature. Phase analysis and the refinement of the lattice parameters were performed using the Rietveld technique with Rietica software [25]. The temperature dependence of magnetization and magnetization isotherms at selected temperatures in the vicinity of their ordering temperatures were measured with a super-conducting quantum interference device (SQUID) magnetometer.

#### 3. Results and Discussion

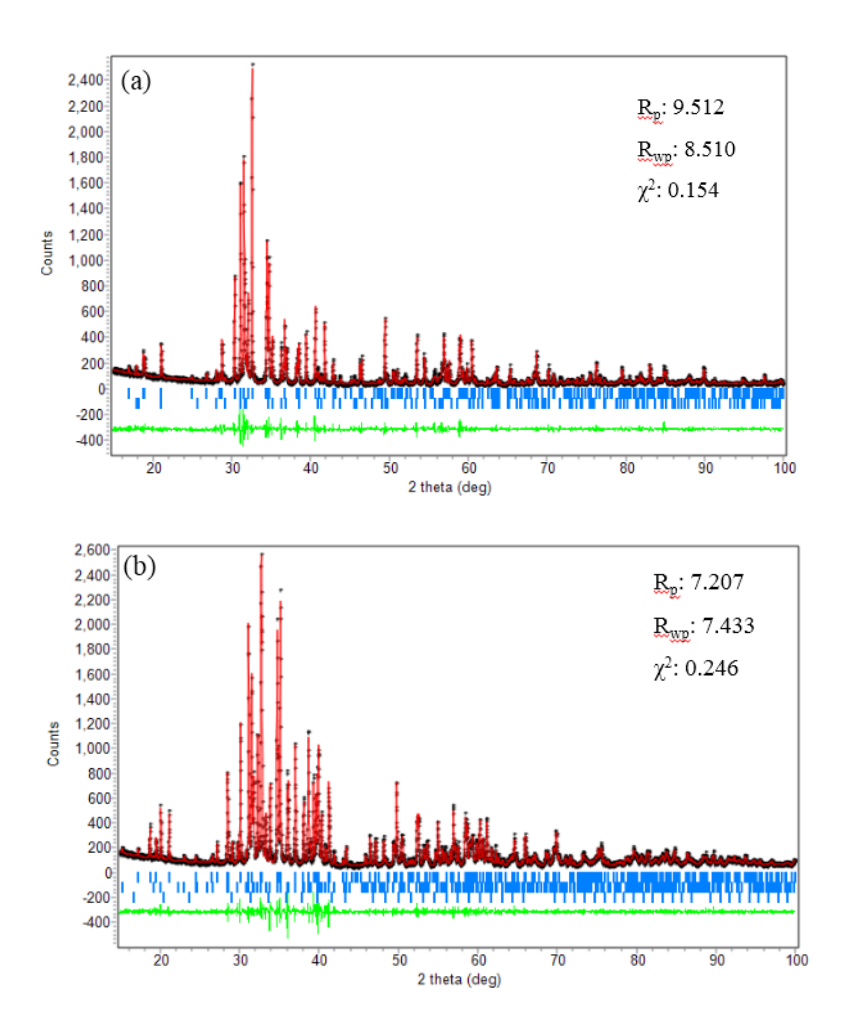


Fig. 1 X-ray diffractograms at room temperature of powdered Ho<sub>3</sub>M (M = Rh, Ru) using Cu-*ka*<sub>1</sub> radiation. The difference between measured (crosses) and calculated (solid line) intensities is plotted in the bottom. The set of blue bars corresponds to calculated Bragg positions of the involved phases.

In Ho-Rh binary diagram, Ho<sub>3</sub>Rh melts congruently near 1500 °C and its neighboring phases at room temperature are Ho and Ho<sub>7</sub>Rh<sub>3</sub>. However, in Ho-Ru diagram, Ho<sub>3</sub>Ru partially melts near 1250 °C and its neighboring phases at room temperature are Ho and Ho<sub>5</sub>Ru<sub>2</sub>. Fig. 1 shows the XRD patterns together with the Rietveld refinement results of the as-cast stoichiometric Ho<sub>3</sub>Rh and Ho<sub>3</sub>Ru alloys at

room temperature. Unexpectedly, it can be seen from Fig. 1 (a) that Ho<sub>3</sub>Rh and the Ho<sub>7</sub>Rh<sub>3</sub> phases coexist in the Ho<sub>3</sub>Rh sample even though the congruent solidification behavior as suggested in the Ho-Rh diagram. Fig. 1 (b) indicates three phases, Ho<sub>3</sub>Ru, Ho<sub>5</sub>Ru<sub>2</sub>, and trace of Ho<sub>2</sub>O<sub>3</sub>, are present in the Ho<sub>3</sub>Ru sample. The presence of the holmium oxide may be related to the lower purity of Ru raw materials compared with Rh. The refinement results of the phase proportions, cell parameters, and unit cell volume (*V*) are depicted in Table 1. The cell parameters of Ho<sub>3</sub>Rh, Ho<sub>7</sub>Rh<sub>3</sub>, Ho<sub>3</sub>Ru, and Ho<sub>5</sub>Ru<sub>2</sub> agree well with the literature data [22,23,26].

Table 1. The Rietveld refinement results of the phase proportion, lattice parameters (a, b, c), and unit cell volume (V) of the component phases in Ho<sub>3</sub>Rh and Ho<sub>3</sub>Ru alloys.

Sample	Phase	Proportion	Lattice Parameters (Å)			Cell Volume
		(wt. %)	а	b	С	$(\mathring{A}^3)$
Ho <sub>3</sub> Rh	Ho <sub>3</sub> Rh	78.23	7.1077(1)	9.3216(3)	6.2596(2)	414.73(3)
	$Ho_7Rh_3$	21.77	9.7044(2)	9.7044(2)	6.1019(1)	497.66(3)
Ho₃Ru	Ho <sub>3</sub> Ru	60.49	7.2525(2)	9.0903(1)	6.2420(1)	411.53(2)
	$Ho_5Ru_2$	38.54	15.5638(1)	6.2509(2)	7.2724(1)	701.84(3)
	$Ho_2O_3$	0.97	10.6278(2)	10.6278(2)	10.6278(2)	1200.41(2)

Figure 2 (a) and (b) show the temperature dependence of magnetizations (*M-T*) measured with 100 Oe applied field on heating after zero-field-cooled (ZFC) and on the following field-cooling (FC) process for the Ho<sub>3</sub>Rh and Ho<sub>3</sub>Ru alloys, respectively. For the ZFC curve, two distinct cusps at 34 and 22 K can be observed in Fig 2 (a). In the Ho<sub>3</sub>Rh single crystal, a transition near 35 K occurs in the thermal variations of the magnetization along the [100], [010], [001], and [2-2-1] directions. Therefore, the transition near 34 K can be ascribed to the ordering of Ho<sub>3</sub>Rh phase from the paramagnetic to the canted ferromagnetic. In the Ho<sub>7</sub>Rh<sub>3</sub> single crystal, a Curie temperature presents in the AC magnetic susceptibility near 24 K <sup>[27]</sup>. Thus, the

transition about 22 K is from the ferromagnetic contribution of the Ho<sub>7</sub>Rh<sub>3</sub> phase in the sample. Similarly, two cusps can also be observed in the FC curve and they occur at 32 K and 19 K, respectively, which are a little lower than those in the ZFC curve. It is worth mention that the reorientation transition of Ho<sub>3</sub>Rh phase occurring around 25 K may be masked by the Curie temperature of Ho<sub>7</sub>Rh<sub>3</sub> phase due to its small change in the magnetization. Shown in Fig. 2 (a) inset is the reciprocal susceptibility of the Ho<sub>3</sub>Rh alloy plotted from the ZFC data. The reciprocal susceptibility above 50 K increases linearly with increasing temperature and follows the Curie–Weiss behavior. The paramagnetic Curie temperature  $\theta_C$  of 39 K can be obtained after fitting the linear part. The positive intercept with the horizontal axis strongly suggests the dominant ferromagnetic interaction in the Ho<sub>3</sub>Rh primary phase in the sample.

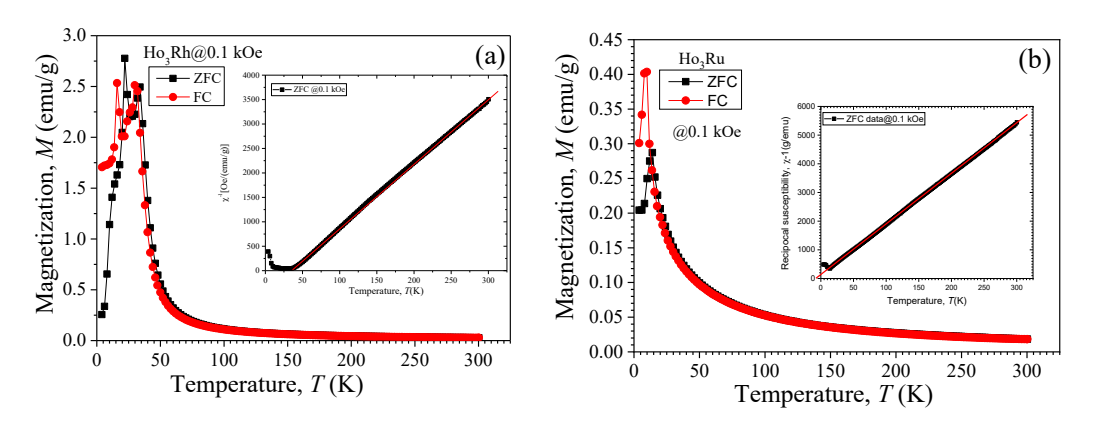


Fig. 2 Temperature dependence of magnetization of  $Ho_3Rh$  (a) and  $Ho_3Ru$  (b) alloys in ZFC and FC modes. The inset shows the reciprocal susceptibility ( $\chi^{-1}$ ) plotted by using the ZFC data.

As shown in Fig. 2 (b), in spite of the multiple-phase structure, only one cusp can be observed and the corresponding temperatures are found to be 14.0 and 9.8 K, for the ZFC and FC curves, respectively. It was reported by Y. Hanaue and coworkers that Ho<sub>3</sub>Ru and Ho<sub>5</sub>Ru<sub>2</sub> phases order antiferromagnetically and ferromagnetically at 13 K and 7 K, respectively <sup>[24]</sup>. However, the transition of Ho<sub>5</sub>Ru<sub>2</sub> phase is not detected in

our measurements due to its low transition temperature. Shown in Fig. 2 (b) inset is the reciprocal susceptibility of the Ho<sub>3</sub>Ru alloy plotted from the ZFC data. The reciprocal susceptibility above 20 K obeys the Curie–Weiss behavior and the paramagnetic Curie temperature  $\theta_C$  is -8 K. The negative intercept with the temperature indicates the dominant antiferromagnetic interaction in the Ho<sub>3</sub>Ru phase.

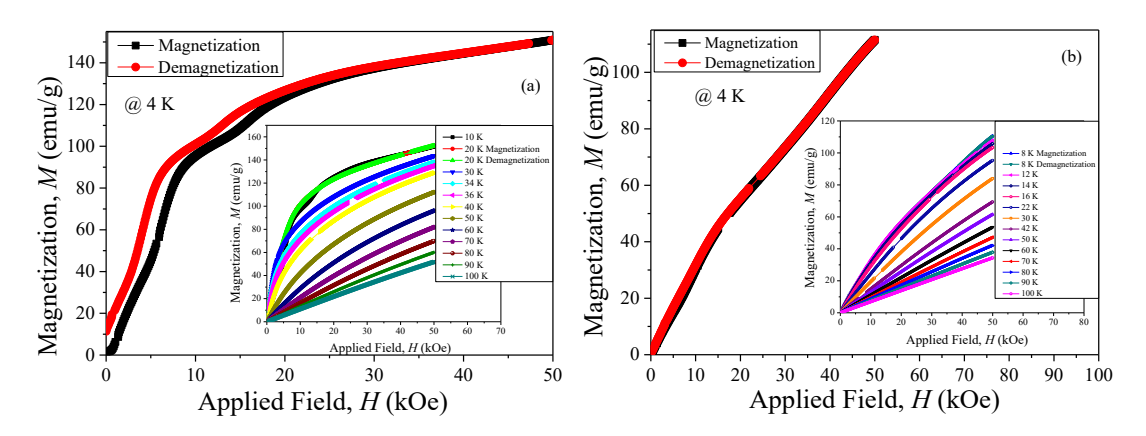


Fig. 3 Magnetization isotherms of Ho<sub>3</sub>Rh (a) and Ho<sub>3</sub>Ru (b) alloys under applied field up to 50 kOe.

The magnetization and demagnetization of the as-cast Ho<sub>3</sub>Rh alloy measured at 4 K under an applied field up to 50 kOe are shown in Fig. 3 (a). Firstly, the magnetization increases rapidly with increasing the applied field to 10 kOe. Then, in the range between 10 and 20 kOe, a step-like change in the magnetization can be observed. Finally, above 20 kOe, the magnetization goes up slowly and linearly, which reflects the antiferromagnetic interaction in the sample. When the field reaches 50 kOe the magnetization is 150 emu/g, which corresponds to 5.3  $\mu_B/\text{Ho}^{3+}$  and is far lower than the theoretical value of 10.0  $\mu_B$ . In Ho<sub>3</sub>Rh single crystal, a metamagnetic transition takes place between 15 and 20 kOe in the magnetization at 4.2 K along the [001] direction. In Ho<sub>7</sub>Rh<sub>3</sub> single crystal, delicate metamagnetic transitions can also be observed at 4 K when the applied field exceeds 20 and 30 kOe for the *a*-axis and *b*-

axis, respectively <sup>[27]</sup>. Therefore, the metamagnetic transition observed at 4 K in Fig.3 (a) can be understood by the main contribution of Ho<sub>3</sub>Rh phase in the sample. In addition, the demagnetization cannot retrace the magnetization when the field is lower than 20 kOe and magnetic hysteresis happens. The residual magnetization is about 10 emu/g when the field returns to zero. Both the hysteresis and residual magnetization verify the ferromagnetic component in the sample. The magnetization at 10 K behaves similarly as the isothermals at 4 K. When the temperature is higher than 20 K all the demagnetization can follow the magnetization and no hysteresis can be observed.

As can be seen from Fig.3 (b), for the Ho<sub>3</sub>Ru alloy, the magnetization at 4 K increases almost linearly with the applied field. When the field reaches 50 kOe, the magnetization is only 120 emu/g, which is far lower than the saturation value 280 emu/g. Nonetheless, one inflection point can be observed near 15 kOe field and it disappears when the temperature is higher than 8 K. Consider the multiple-phase structure in Ho<sub>3</sub>Ru sample, the presence of the inflection point may be associated with the ferromagnetic phase Ho<sub>5</sub>Ru<sub>2</sub> with transition temperature near 7 K. When temperature is above 8 K, all the isotherms follow the typical antiferromagnetic magnetization characteristic of linear increasing with field.

Figure 4 is the Arrott plot of Ho<sub>3</sub>Rh sample at different temperatures. According to the Banerjee criterion <sup>[28]</sup>, a magnetic transition is expected to be of the first order if the slope of the Arrott plot is negative, whereas it will be of the second order if the slop is positive. When the temperature is lower than 10 K the negative slop of the

Arrott plot is present, which confirms the first-order characteristic of the field-induced AFM-to-FM metamagnetic transition observed in the isotherms.

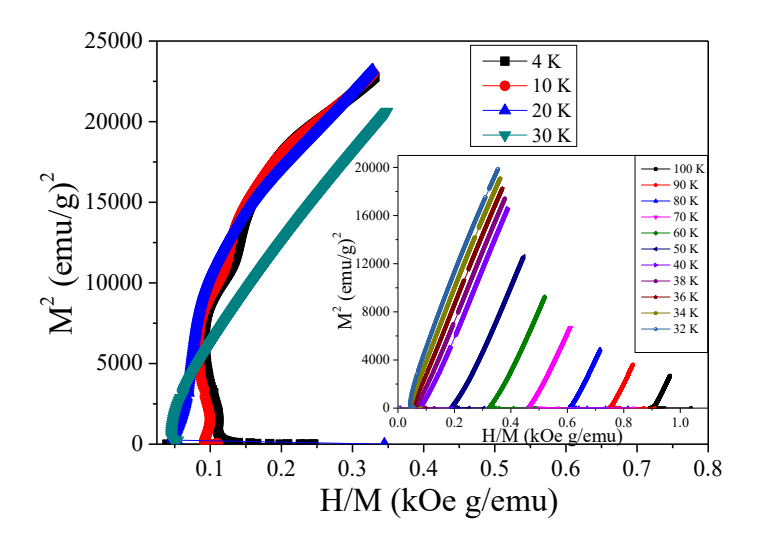


Fig. 4 Arrott plot of Ho<sub>3</sub>Rh in temperature range of 4-100 K.

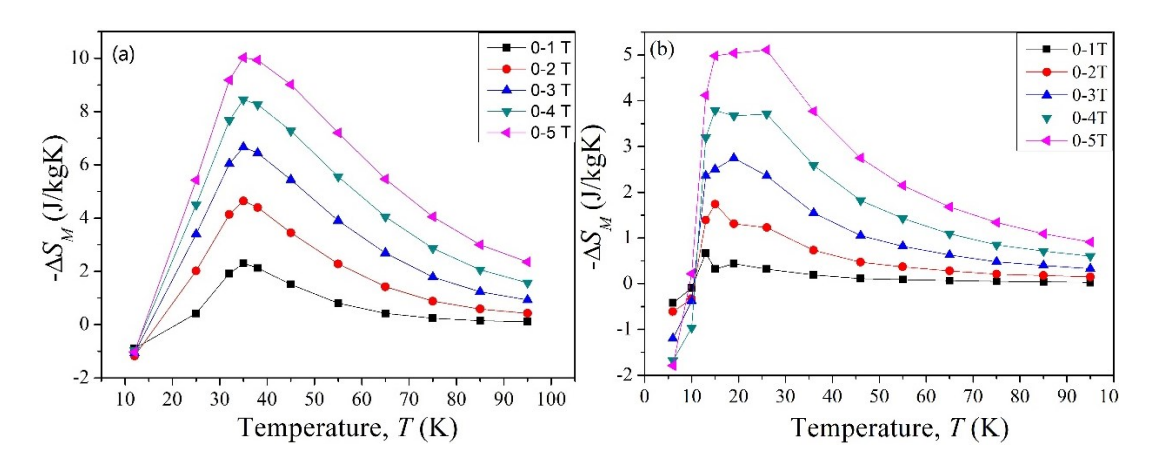


Fig. 5 Temperature dependence of magnetic entropy changes  $(-\Delta S_M)$  of the Ho<sub>3</sub>Rh (a) and Ho<sub>3</sub>Ru (b) alloys

The magnetic entropy changes  $(-\Delta S_M)$  as a function of temperature for the Ho<sub>3</sub>Rh and Ho<sub>3</sub>Ru alloys under various applied field change are shown in Fig.5 (a) and Fig.5 (b), respectively. They were calculated from the magnetization isotherms in Fig. 3 (a) and Fig. 3 (b) by using the Maxwell relation <sup>[29]</sup> as follows.

$$\Delta S_M(T, \Delta H) = S_M(T, H) - S_M(T, 0) = \int_0^H \left(\frac{\partial M}{\partial T}\right)_H dH. \tag{1}$$

It is found that the values of  $-\Delta S_{\rm M}$  for Ho<sub>3</sub>Rh are negative when the temperatures are below 14 K, which is from the antiferromagnetic contribution of the component phases at low temperature in Fig. 5 (a). However, they become positive with increasing of temperature due to the ferromagnetic interaction near the transition temperatures of the phases Ho<sub>7</sub>Rh<sub>3</sub> and Ho<sub>3</sub>Rh. It can be seen from Fig. 5 (a) that the maximal values of the magnetic entropy change ( $-\Delta S_{\text{M-max}}$ ) are 2.3, 4.6, 6.7, 8.4, and 10.0 J/kg K occurring around 36 K at field changes  $\Delta H = 10, 20, 30, 40, \text{ and } 50 \text{ kOe},$ respectively. Despite the component of antiferrometism in the sample, the large rare earth content and thus the large change in the magnetization near the ordering temperature can interpret the moderate  $-\Delta S_{\rm M}$  in the sample with canted ferromagnetic main phase. Fig. 5 (b) shows the -△S<sub>M</sub> of the Ho<sub>3</sub>Ru sample in a different magnetic field change. The maximum  $-\Delta S_{\rm M}$  approach 0.6, 1.7, 2.7, 3.8, and 5.1 J/kg K at field changes  $\Delta H = 10, 20, 30, 40,$  and 50 kOe, respectively, which are less than that of the Ho<sub>3</sub>Rh sample and other ferromagnetic compounds with ordering temperature near 20 K. The refrigerant capacity RC, the amount of heat that can be transferred between the hot and cold reservoirs in an ideal refrigerant cycle, can be calculated as follows<sup>[30]</sup>:

$$RC = \int_{T_1}^{T_2} |\Delta S_M| dT, \tag{2}$$

where  $T_1$  and  $T_2$  are the temperatures corresponding to the both sides of the full width at half maximum of the  $-\Delta S_{\rm M}$  versus T curve ( $\delta T_{FWHM}$ ). It is estimated that the value of RCs are 320 J/kg and 145 J/kg for a field change of 50 kOe for the Ho<sub>3</sub>Rh and Ho<sub>3</sub>Ru alloys, respectively. Although the  $-\Delta S_{\rm M}$  is much lower than the first order MCE

materials, the RC of Ho<sub>3</sub>Rh alloy is superior and competitive. For example, the  $-\Delta S_{\rm M}$  of the first-order ErCo<sub>2</sub> alloy is as large as 28.5 J/kg K near the Curie temperature of 35 K. However, its RC is only 250 J/kg [31].

#### 4. Conclusions

In the present work, we have studied the structure, magnetic properties, and magnetocaloric effect (MCE) of Ho<sub>3</sub>M (M= Rh, Ru) compounds. Both the polycrystalline samples are not single-phase structure. Ho<sub>3</sub>Rh alloy possesses two phases, Ho<sub>3</sub>Rh and Ho<sub>7</sub>Rh<sub>3</sub>, and the Ho<sub>3</sub>Ru alloy consists of three phases, Ho<sub>3</sub>Ru, Ho<sub>5</sub>Ru<sub>2</sub>, and Ho<sub>2</sub>O<sub>3</sub>. Two ferromagnetic transitions near 34 and 22 K corresponds to the ordering temperatures of Ho<sub>3</sub>Rh and Ho<sub>7</sub>Rh<sub>3</sub> phases, respectively, in the Ho<sub>3</sub>Rh polycrystalline sample. Only one Neel transition temperature can be observed near 14 K despite the multiphase structure for the Ho<sub>3</sub>Ru sample. The moderate - $\Delta$ S<sub>M</sub> and large RC of 10.0 J/kg K and 320 J/kg for the Ho<sub>3</sub>Rh alloy with canted magnetic structure are obtained with magnetic field change of 50 kOe. In contrast, the Ho<sub>3</sub>Ru alloy is antiferromagnetic and its - $\Delta$ S<sub>M</sub> and RC are only 5.1 J/kg K and 145 J/kg with  $\Delta$ H = 50 kOe. The excellent magnetocaloric performance indicates the applicability of Ho<sub>3</sub>Rh as an appropriate candidate for magnetic refrigerant near liquid-hydrogen temperature.

## Acknowledgments

This work was supported by the National Natural Science Foundation of China (No. No. 51750110501).

#### References

- [1] Liu J L, Chen Y C, Guo F S, et al. Recent advances in the design of magnetic molecules for use as cryogenic magnetic coolants[J]. Coordination Chemistry Reviews, 2014, 281: 26-49.
- [2] Sessoli R. Chilling with magnetic molecules[J]. Angewandte Chemie International Edition, 2012, 51(1): 43-45.
- [3] Zheng Y Z, Zhou G J, Zheng Z, et al. Molecule-based magnetic coolers[J]. Chemical Society Reviews, 2014, 43(5): 1462-1475.
- [4] Zheng X Y, Kong X J, Zheng Z, et al. High-nuclearity lanthanide-containing clusters as potential molecular magnetic coolers[J]. Accounts of chemical research, 2018, 51(2): 517-525.
- [5] GschneidnerJr K A, Pecharsky V K, Tsokol A O. Recent developments in magnetocaloric materials[J]. Reports on progress in physics, 2005, 68(6): 1479.
- [6] Shen B G, Sun J R, Hu F X, et al. Recent progress in exploring magnetocaloric materials[J]. Advanced Materials, 2009, 21(45): 4545-4564.
- [7] Pecharsky V K, Gschneidner Jr K A. Advanced magnetocaloric materials: What does the future hold?[J]. International Journal of Refrigeration, 2006, 29(8): 1239-1249.
- [8] Hu F, Shen B, Sun J, et al. Influence of negative lattice expansion and metamagnetic transition on magnetic entropy change in the compound LaFe<sub>11.4</sub>Si<sub>1.6</sub>[J]. Applied Physics Letters, 2001, 78(23): 3675-3677.
- [9] Wada H, Tanabe Y. Giant magnetocaloric effect of MnAs<sub>1-x</sub>Sb<sub>x</sub>[J]. Applied physics letters, 2001, 79(20): 3302-3304.
- [10] Tegus O, Brück E, Buschow K H J, et al. Transition-metal-based magnetic refrigerants for room-temperature applications[J]. Nature, 2002, 415(6868): 150.
- [11] He A, Svitlyk V, Mozharivskyj Y. Synthetic approach for (Mn, Fe)<sub>2</sub>(Si, P) magnetocaloric materials: purity, structural, magnetic, and magnetocaloric properties[J]. Inorganic chemistry, 2017, 56(5): 2827-2833.
- [12] Hu F, Shen B, Sun J. Magnetic entropy change in Ni<sub>51.5</sub>Mn<sub>22.7</sub>Ga<sub>25.8</sub> alloy[J]. Applied Physics Letters, 2000, 76(23): 3460-3462.
- [13] Hu F, Shen B, Sun J, et al. Large magnetic entropy change in a Heusler alloy

- Ni<sub>52.6</sub>Mn<sub>23.1</sub>Ga<sub>24.3</sub> single crystal[J]. Physical Review B, 2001, 64(13): 132412.
- [14] Krenke T, Duman E, Acet M, et al. Inverse magnetocaloric effect in ferromagnetic Ni–Mn–Sn alloys[J]. Nature materials, 2005, 4(6): 450.
- [15] Talik E, Klimczak M. Giant magnetocaloric effect in Tb<sub>3</sub>Rh[J]. Journal of Alloys and Compounds, 2009, 486(1-2): L30-L33.
- [16] Tripathy S K, Suresh K G, Nigam A K. A comparative study of the magnetocaloric effect in Gd<sub>3</sub>Co and Gd<sub>3</sub>Ni[J]. Journal of magnetism and magnetic materials, 2006, 306(1): 24-29.
- [17] Kumar P, Suresh K G, Nigam A K. Magnetothermal effect in Gd<sub>3</sub>Rh[J]. Journal of Applied Physics, 2011, 109(7): 07A909.
- [18] Monteiro J C B, dos Reis R D, Gandra F G. The physical properties of Gd<sub>3</sub>Ru: A real candidate for a practical cryogenic refrigerator[J]. Applied Physics Letters, 2015, 106(19): 194106.
- [19] Li B, Du J, Ren W J, et al. Large reversible magnetocaloric effect in Tb<sub>3</sub>Co compound[J]. Applied Physics Letters, 2008, 92(24): 242504.
- [20] Monteiro J C B, Lombardi G A, dos Reis R D, et al. Heat flux measurements of Tb<sub>3</sub>M series (M= Co, Rh and Ru): Specific heat and magnetocaloric properties[J]. Physica B: Condensed Matter, 2016, 503: 64-69.
- [21] Shen J, Zhao J L, Hu F X, et al. Magnetocaloric effect in antiferromagnetic Dy<sub>3</sub>Co compound[J]. Applied Physics A, 2010, 99(4): 853-858.
- [22] Talik E, Mydlarz T, Kusz J, et al. Magnetic properties of Ho<sub>3</sub>Rh single crystals[J]. Journal of alloys and compounds, 2002, 336(1-2): 29-35.
- [23] Palenzona A. The crystal structure of the rare earth rich ruthenium compounds R<sub>3</sub>Ru and R<sub>5</sub>Ru<sub>2</sub>[J]. Journal of the Less Common Metals, 1979, 66(2): P27-P33.
- [24] Hanaue Y, Ishiyama K, KIMURA E, et al. Development of Rare Earth-Ruthenium Intermetallic Compounds for Use as Regenerator Materials[J]. TEION KOGAKU (Journal of Cryogenics and Superconductivity Society of Japan), 1996, 31(4): 156-161.
- [25] Hunter B A, Howard C J. Rietica; Australian Nuclear Science and Technology Organization: Menai[J]. 2000.
- [26] Olcese G L. Crystal structure and magnetic properties of some 7: 3 binary phases between

lanthanides and metals of the 8th group[J]. Journal of the Less Common Metals, 1973, 33(1): 71-81.

- [27] Tsutaoka T, Obata K, Sherstobitov AA, et al. Magnetic order, phase transitions and electrical resistivity of Ho7Rh3 single crystals[J]. Journal of Alloys and Compounds, 2016, 654: 126-132.
- [28] Banerjee B K. On a generalised approach to first and second order magnetic transitions[J]. Physics letters, 1964, 12: 16-17.
- [29] N.A.de Oliveira, P.J.von Ranke. Magnetocaloric effect around a magnetic phase transition[J]. Phys. Rev., 2008, 77(21):214439.
- [30] GschneidnerJr K A, Pecharsky V K, Tsokol A O. Recent developments in magnetocaloric materials[J]. Reports on progress in physics, 2005, 68(6): 1479.
- [31] Balli M, Fruchart D, Gignoux D. Magnetic behaviour and experimental study of the magnetocaloric effect in the pseudobinary Laves phase Er<sub>1-x</sub>Dy<sub>x</sub>Co<sub>2</sub>[J]. Journal of Alloys and Compounds, 2011, 509(9): 3907-3912.